In-plane anisotropy of the optical properties of $(In_{0.5}Ga_{0.5}As)_n/(InP)_n$ superlattices

Rita Magri and Stefano Ossicini
Istituto Nazionale per la Fisica della Materia and Dipartimento di Fisica, Università di Modena e Reggio Emilia, Via Campi 213/a, I-41100 Modena, Italy

(Received 7 March 2000; published 2 April 2001)

In this paper we study the electronic and optical properties of $(In_{0.5}Ga_{0.5}As)_n/(InP)_n$ superlattices, where the $Ga_{0.5}In_{0.5}As$ alloy is described both through the virtual crystal approximation (VCA) and through an appropriate ordered ternary structure. By first-principles calculations of the dielectric tensor elements we address the issue of the giant polarization anisotropy of the optical absorption experimentally observed in these superlattices. The magnitude of the anisotropy depends on the splitting between the hole states at the valence band top which is due to the lowering of the overall symmetry to the C_{2v} point group and it is greatly influenced by strain not only at the interfaces but also in the bulk alloy.

DOI: 10.1103/PhysRevB.63.165303 PACS number(s): 73.21.−b, 78.66.Fd

I. INTRODUCTION

''No-common atom'' (NCA) superlattices (superlattices in which the host materials do not share common atoms), constitute an interesting system for exploring the interface related features in the electronic and optical properties of superlattices (SLs) and multiquantum wells (MQWs). This is because in *ideal* NCA systems, such as (InGa)As-InP or InAs-AlSb, there can be two inequivalent interfaces, while in *ideal* ''common atom'' (CA) superlattices, such as (AlGa)As-GaAs, there is always only one kind of interface. This different behavior is shown mainly in the optical properties. The optical transmission spectra of InGaAs-InP MQW structures grown along the [0,0,1] direction display a strong anisotropy of the optical absorption α with respect to the angle θ between the photon polarization and the sample x axis. In particular it has been shown that the absorption is stronger when the photon polarization is along the [1,1,0] direction than when it is along the $[-1,1,0]$ direction for light propagating along the superlattice growth direction. CA MQWs, instead, do not show any polarization anisotropy of the optical absorption.[1–3]

The existence of two subsequent inequivalent interfaces in NCA superlattices leads to a reduction of the crystal field symmetry. While CA MQWs have a D_{2d} point group with eight symmetry operations, in the NCA MQWs that have inequivalent interfaces the symmetry is reduced to a C_{2v} point group which has only four symmetry operations. The C_{2v} point group misses the symmetry operations related to the z-axis inversion that change $z \rightarrow -z$. In a CA superlattice, for example with a common anion, the host materials can be indicated with C_1A and C_2A where A is the common anion and C_1 and C_2 the two cations. In this case the interface is properly identified with a single A plane, and in case of ideal and abrupt geometries, all the interfaces have the same atomic configurations: an A plane with a C_1 plane on one side and a C_2 plane on the other side. At two subsequent interfaces the role of the C_1 and C_2 planes is just reversed. As a consequence the structure has a symmetry plane with respect to the $z \rightarrow -z$ operations. In the NCA superlattices, instead, with ideal and abrupt interfaces between the two C_1-A_1 and C_2-A_2 host materials, the interfaces can be considered constituted by a *couple* of planes. The interface bonds C_1-A_2 and C_2-A_1 are different from the bonds in the two bulk constituents. Moreover, at a C_1-A_1/C_2-A_2 interface, if A_1 is the interface plane, the C_1-A_1 bonds lie in the $\{-1,1,0\}$ plane, while the C_2-A_1 bonds lie in the $\{1,1,0\}$ plane. In the CA superlattices this situation is just compensated at the other interface with the C_2-A_1 bonds in the $\{-1,1,0\}$ plane and the C_1-A_1 bonds in the $\{1,1,0\}$ plane. This compensation does not occur in NCA superlattices because the chemical species forming the bonds themselves are different: there are C_1-A_1 and C_2-A_1 bonds at one interface and C_2-A_2/C_1-A_2 bonds at the other interface. This situation is displayed in Fig. 1. Consequently, the crystal potential is not anymore symmetric with respect to the midpoint of the QW layer for all the rotoinversion operations of the D_{2d} point group changing z into $-z$.

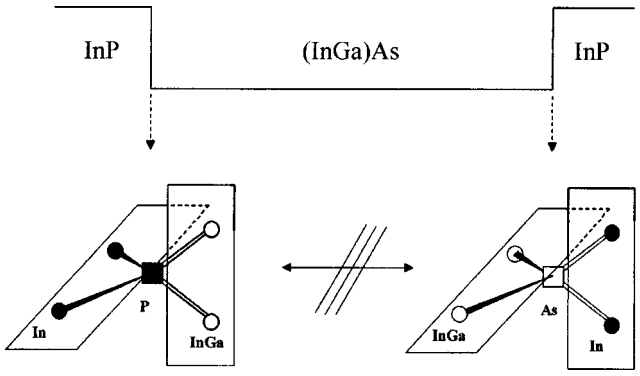

FIG. 1. Scheme of the chemical bond configurations at the interfaces in the (GaIn)As/InP NCA superlattices. Vertical planes indicate (110) planes while horizontal planes indicate (−110) planes. The figure stresses the orientation of the nearest neighbor bonds at the (001) interfaces with respect to the growth [001] direction which is indicated by the two-ended arrow. Indeed changing z to $-z$ does not change the physical description of the infinite system. Only care has to be used into attributing the results for the [110] direction to the $[-110]$ direction and vice versa.

The inequivalence of the (001) interfaces and the related symmetry reduction give rise to the observed polarizarion anisotropy of the optical absorption of the NCA superlattices. This point has been investigated through semiempirical tight binding and envelope function approaches. The polarization anisotropy cannot be predicted by the standard $\mathbf{k}\cdot\mathbf{p}$ theory, in which potential fluctuations on the scale of atomic spacing are not taken explicitly into account. Krebs and Voisin[1] and Ivchenko *et al.*[4] have introduced phenomenological approaches to include a coupling potential at the interfaces into the framework of the $\mathbf{k}\cdot\mathbf{p}$ theory in the envelope function approximation. Both approaches turn out to be substantially equivalent and lead to a mixing of the heavy and light hole states at the zone center and ultimately to a polarization dependence of the optical absorption coefficient. In both cases the magnitude of the mixing depends on parameters whose value is obtained by fitting the experimental data.[5]

Similarly, a semiempirical tight-binding calculation,[3] which includes strain effects at the interfaces but does not take into account a possible superlattice valence band offset asymmetry,[6] finds a partial admixture of the light and heavy characters in the hole wave functions. This calculation finds that, due to the mixing of the light and heavy hole characters, the optical transitions from the upmost valence states to the first conduction state at the zone center are in-plane polarized. This leads to a polarization angle dependence of the oscillator strengths and, ultimately, to a polarization dependence of the absorption spectrum.

These theoretical results based on semiempirical approaches agree qualitatively with the experiment but the predicted polarization rates

$$P(h\nu)=\frac{\alpha_{110}-\alpha_{\bar{1}10}}{\alpha_{110}+\alpha_{\bar{1}10}} \tag{1}$$

are consistently smaller than the experimental ones and depend critically on the value assigned to adjustable parameters.

Our *ab initio* calculations[7] have clarified the relation between the global symmetry of the system, the dielectric tensor elements, and the conditions leading to the observed in-plane polarization anisotropy. Now the aim of this paper is (1) to assess separately the different effects contributing to the polarization anisotropy of the optical absorption in $(Ga_{0.5}In_{0.5}As)/(InP)$ without having to put into the calculation *ad hoc* parameters and (2) to shed light into the link between the microscopical configuration of the atomic bonds both at the superlattice interfaces and in the $Ga_{0.5}In_{0.5}As$ alloy bulk and the dielectric tensor.

II. SUPERLATTICE SYMMETRY AND THE DIELECTRIC TENSOR

We start our study by considering the imaginary part of the dielectric function which is directly related to the optical absorption:

$$\alpha(\omega)=\frac{\omega}{n(\omega)c}\epsilon_2(\omega). \tag{2}$$

At the first order perturbation theory, in the dipole approximation:

$$\epsilon_2(\omega)=\frac{8\pi^2e^2}{\omega^2m^2V}\sum_{v,c}\sum_{k}|\vec{e}\cdot\vec{P}_{v,c}(k)|^2 \times\delta[E_c(k)-E_v(k)-\hbar\omega], \tag{3}$$

where $\vec{P}_{v,c}(k)=\langle v,k|\vec{P}|c,k\rangle$ is the matrix element of the optical transition between the valence state $|v,k\rangle$ and the conduction state $|c,k\rangle$. V is the unit cell volume over which $\epsilon_2(\omega)$ is normalized. The optical absorption of an infinite system does not depend on the chosen dimension of the unit cell.

To describe the optical anisotropy it is better to work with the dielectric tensor

$$\epsilon_{i,j}(\omega)=\frac{8\pi^2e^2}{\omega^2m^2V}\sum_{v,c}\sum_{k}[P_{v,c}(k)]_i^*[P_{v,c}(k)]_j \times\delta[E_c(k)-E_v(k)-\hbar\omega], \tag{4}$$

where $i,j=x,y,z$ and $[P_{v,c}(k)]_x=\langle v,k|P_x|c,k\rangle$. For a wave traveling along the z axis, the general direction of the polarization vector in the (001) plane can be indicated with $\vec{e}=(\cos\theta,\sin\theta,0)$, where θ is the angle between the polarization direction and the [100] axis. This gives

$$\epsilon_2(\omega,\theta)=\epsilon_{xx}(\omega)\cos^2\theta+\epsilon_{xy}(\omega)\sin 2\theta+\epsilon_{yy}(\omega)\sin^2\theta. \tag{5}$$

Denoting $\epsilon_{yy}(\omega)=\epsilon_{xx}(\omega)+\delta\epsilon_{xx,yy}(\omega)$, we obtain

$$\epsilon_2(\omega,\theta)=\epsilon_{xx}(\omega)+\delta\epsilon_{xx,yy}(\omega)\sin^2\theta+\epsilon_{xy}(\omega)\sin 2\theta. \tag{6}$$

From this expression we see that ϵ_2, the absorption, depends on θ, the in-plane polarization direction, if (1) the diagonal elements ϵ_{xx} and ϵ_{yy} of the dielectric tensor are different $[\delta\epsilon_{xx,yy}(\omega)\neq 0$ and/or 2] the off-diagonal element ϵ_{xy} is different from zero. Without a direct calculation of the dielectric tensor elements we can nevertheless derive the relations among the dielectric tensor elements simply by looking at the symmetry of the system. Now the dipole oscillator matrix elements transform under the operation of the crystal symmetry group as[8]

$$\vec{P}_{v,c}(R^{-1}\vec{k})=e^{i\gamma}R\vec{P}_{v,c}(\vec{k}), \tag{7}$$

where R indicates a symmetry operation of the crystal point group. By applying Eq. (7) we reduce the summation in Eq. (4) to the k points in the irreducible wedge of the Brillouin zone (IBZ) and determine the elements of the dielectric tensor for the CA (D_{2d}) and NCA (C_{2v}) crystal structures. We report the results in Table I. We see that for NCA SLs and MQWs grown along the [001] direction, having the C_{2v} symmetry, $\delta\epsilon_{xx,yy}(\omega)$ is always zero but $\epsilon_{xy}(\omega)$ is expected to be *different* from zero. Thus, the observed anisotropy of the NCA (001) grown SLs is due to the off-diagonal xy element of the dielectric tensor which is different from zero.

TABLE I. Dielectric tensor elements for CA and NCA multiquantum wells. Here $K=8\pi^2e^2/\omega^2m^2V$. δ stays simply for $\delta[E_c(k)-E_v(k)-\hbar\omega]$. The summation over k is intended only over the IBZ.

Dielectric tensor elements	CA (D_{2d})	NCA (C_{2v})
$\epsilon_{xx}(\omega)=\epsilon_{yy}(\omega)$	$K\Sigma_{v,c}\Sigma_k 4(P_x^*P_x+P_y^*P_y)\delta$	$K\Sigma_{v,c}\Sigma_k 2(P_x^*P_x+P_y^*P_y)\delta$
$\epsilon_{zz}(\omega)$	$K\Sigma_{v,c}\Sigma_k 8P_z^*P_z\delta$	$K\Sigma_{v,c}\Sigma_k 4P_z^*P_z\delta$
$\epsilon_{xy}(\omega)=\epsilon_{yx}(\omega)$	0	$K\Sigma_{v,c}\Sigma_k 2(P_y^*P_x+P_x^*P_y)\delta$
$\epsilon_{xz}(\omega)=\epsilon_{zx}(\omega)$	0	0
$\epsilon_{yz}(\omega)=\epsilon_{zy}(\omega)$	0	0

In fact $\Delta\epsilon(\omega)$ which is the difference between the absorption for $\vec{e}=[110]$ ($\theta=\pi/4$) and that for $\vec{e}=[\bar{1}10]$, ($\theta=-\pi/4$), is given by [using Eq. (6)]

$$\Delta\epsilon(\omega)=\epsilon_2\left(\omega,\frac{\pi}{4}\right)-\epsilon_2\left(\omega,-\frac{\pi}{4}\right)=2[\epsilon_{xy}(\omega)]. \qquad (8)$$

III. MODELS FOR THE $Ga_{0.5}In_{0.5}As$ RANDOM ALLOY

We have used two approximations to model the pseudobinary alloy $(In_{0.5}Ga_{0.5})As$. The first model is the commonly used simple virtual crystal approximation (VCA) where a virtual cation M has been simulated by averaging the In and Ga pseudopotentials $M=(Ga_{0.5}In_{0.5})$. In this approximation the random $(In_{0.5}Ga_{0.5})As$ alloy is described through a *binary* compound, MAs, and more realistic descriptions of the compositional disorder in the alloy constituent, which could lead to a further reduction of the superlattice symmetry, are not taken into account. We analyze first the electronic and optical properties of the $(MAs)_n/(InP)_n$ superlattices because we want to study separately the effects due to strain at the interfaces from the additional effects due to the compositional disorder inside the bulk of the random $(In_{0.5}Ga_{0.5})As$ constituent.

The second model is the ordered true ternary ''special quasirandom structure'' SQS-4.[9] This ordered structure is the structure with *only* 4 atoms per unit cell that better mimic the first few radial correlation functions of a perfectly random structure. To our knowledge the random nature of the GaInAs alloy has never been fully addressed. The only other ternary structure used to approximate the alloy was the (001) $(GaAs)_1(InAs)_1$ superlattice[10] which has alternating Ga and In planes along the [001] direction and an higher symmetry. The SQS-4 structure has instead both Ga and In atoms on each 001 cationic plane. The superlattice with the SQS-4 layer has a lower symmetry than the C_{2v} symmetry of the superlattice formed by the two binary zinc blende constituents [i.e., $(MAs)_n/(InP)_n$]. The resulting symmetry is now C_{1h}. The C_{1h} point group is a subgroup of the original C_{2v} group and we obtain the same coupling between X and Y symmetry states leading to $\epsilon_{xy}(\omega)\neq 0$ as for the C_{2v} symmetry. There are also additional couplings between the (X,Y) states and the Z state but they are much smaller than the couplings between the X and Y states, and, since we are here studying the in-plane (i.e., the xy plane) polarization anisotropy of light propagating along the z direction, they are of none effect on the object of our investigations.

For the VCA approximation we consider superlattices $[MAs]_n$-$[InP]_n$ with $n=12$ and $n=6$ (corresponding to quantum wells 18 and 36 Å wide, respectively) which are shorter than the MQWs grown by metal organic chemical deposition reported in the experimental literature, which all have thicknesses ranging between 45 and 145 Å, but are long enough to separate to an acceptable degree the contributions coming from the two different interfaces. For the SQS-4 approximation we consider a superlattice with period $n=6$. For each layer material we consider an even number of monolayers. Thus the superlattices have two inequivalent interfaces: one (GaIn)P and one InAs interface per unit cell.

In our study we consider superlattices whose period n is very small compared to λ the characteristic wavelength of the optical radiation. Thus, the radiation does not resolve the single superlattice layers and the possible change of the polarization across the interfaces is not an important issue in this case.

IV. METHOD OF CALCULATION

To quantify the group theory predictions we have calculated the electronic and optical properties of a $(In_{0.5}Ga_{0.5})As$-InP superlattice within a first-principles approach. The calculation has been performed in the self-consistent density functional theory (DFT) with the local density approximation (LDA), using nonlocal norm-conserving pseudopotentials.[11] The pseudopotentials are not separable and include scalar relativistic effects and nonlinear core corrections.[12] The Ceperley Alder form[13] for the exchange and correlation energy has been used. The superlattice wave functions have been expanded in plane waves with an energy cutoff 12 Ry. For the results we are interested in here this cutoff is fully adequate as we have checked performing calculations with higher cutoffs on smaller period structures.

This cutoff (and a smaller one 9 Ry.) has been used (with similar pseudopotentials) in the literature to study the electronic properties (in particular the valence band offset) of the $(Ga_{0.5}In_{0.5}As)/(InP)$ superlattices.[10,14,15] The agreement with these previous calculations is good. Thus, we feel that the electronic properties of the superlattices, which are the starting point of the analysis of the optical transitions, are well described.

In the VCA scheme, we obtain for the binary MAs system an equilibrium lattice parameter $a=11.0235$ a.u. and a bulk modulus $B=79$ GPa, while for InP $a=11.0256$ a.u. [a

$=5.83$ Å, to be compared with the experimental value 5.86 Å (Ref. 16)] and $B=77$ GPa [experimental value 72 GPa (Ref. 16)]. Thus, the two binaries can be considered lattice matched (as they are experimentally), the calculated mismatch being less than 0.02%. As a consequence, when InP is grown on ($Ga_{0.5}In_{0.5}As$) (or vice versa) the two bulk systems are not strained. The interface bonds instead are different: In-As bonds at one interface and M-P bonds at the other interface. For the calculations on the corresponding binary systems we find $a=11.395$ a.u. [6.03 Å, experimental value 6.05 Å (Ref. 16)] and $B=61$ GPa [experimental value 58 GPa (Ref. 16)] for InAs, while for the hypothetical binary MP we find $a=10.688$ a.u. (5.66 Å). These results on the binary systems suggest that the In-As bonds, while constrained to the common InP and MAs lateral dimension, will elongate along the z direction to reach a bond distance closer to their bulk value. The M-P bonds at the other interface (see Fig. 1) will shorten accordingly.

To study the effects of the interfacial strain on the optical anisotropy of MAs/InP superlattices we consider separately two cases. We study first the simplest possible situation in which we neglect spin-orbit interaction effects and the elastic strain effects at the interfaces. Under these assumptions only the chemical difference of the constituent atoms at the interfaces is taken into account. This situation is obviously unrealistic since the strain at the interface contributes considerably to the crystal potential antisymmetry along the z axis. Then, the atoms are allowed to relax to their equilibrium positions, keeping fixed the cell dimension along the z axis to $z=na$, where n is the superlattice period and a the common equilibrium lattice constant of InP and MAs. The resulting geometry is very similar to that proposed in Ref. 14. The bond lengths at the two interfaces are closer to their bulk values $d_{\text{In-As}}$ and $d_{\text{M-P}}$. The relaxation does not relieve completely the strain at the interfaces that are considerably strained while the strain in the bulk is very small. This atomic configuration corresponds to a bond length parameter at the interfaces $\varepsilon=0.06$. Thus, $d_{\text{In-As}}=d_0(1+\varepsilon)$ and $d_{(\text{M})\text{-P}}=d_0(1-\varepsilon)$, where d_0 is the calculated common bond length of the two lattice-matched constituents. The resulting total energy is reduced by 64 meV and an inspection of the atomic forces shows that the system is indeed relatively close to an energy minimum.

Also for the SQS-4 we have studied separately: (1) the ''ideal'' configuration where the atoms are kept fixed at their ideal zinc blende sites and (2) a relaxed configuration where the atoms are at their minimum energy sites. In this second case the resulting configuration is very distorted and the strain is transmitted through the entire InP layer where some monolayer distances along z are consequently modified. The largest distortions are located at the interfaces with an average bond length parameter (averaged over the In-P and Ga-P bond lengths at the $Ga_{0.5}In_{0.5}$-P interface) $\varepsilon=0.073$ at both interfaces. The plane distances along z are slightly increased in the InP segment and slightly smaller in the SQS-4 $Ga_{0.5}In_{0.5}As$ segment. This is because the superlattice SQS-4/InP is a relatively short superlattice (period $n=6$) and the ordered ternary SQS structure is less efficient in relieving its bulk strain than a true random alloy. The results we obtain from this study have to be considered as relative to two extreme conditions for a real $(Ga_{0.5}In_{0.5}As)_n(InP)_n$ superlattice: a zero bulk strain in the $(MAs)_n(InP)_n$ system and a very large bulk strain in the $(SQS\text{-}4)_n(InP)_n$ system. The real situation will be somewhat in between these two limits.

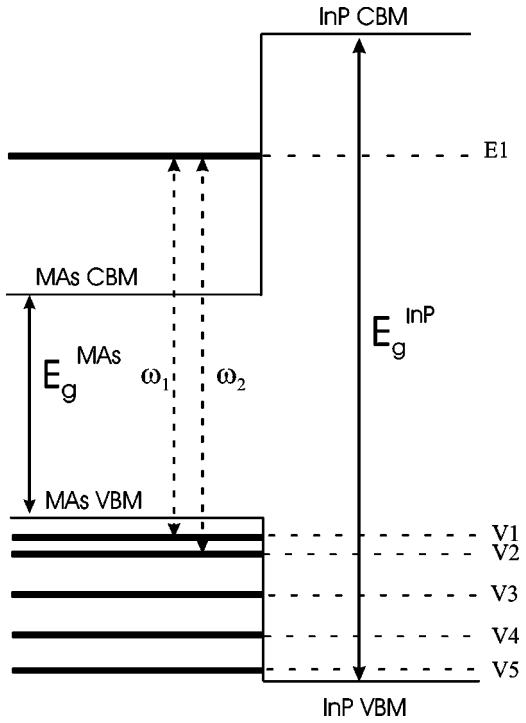

FIG. 2. Diagram scheme of energy levels, band alignment, and interband transitions in $(MAs)_{12}(InP)_{12}$.

V. RESULTS

A. Electronic properties: Confined states and wave functions

In Fig. 2 the scheme of the energy levels which are confined in the hole and electron wells (both located into the $Ga_{0.5}In_{0.5}As$ segment) is given for the $(MAs)_{12}(InP)_{12}$ superlattice. We have calculated a 225 meV valence band offset (VBO) between MAs and InP (without taking into account quasiparticle and spin-orbit effects). Using this value we find that five hole levels are confined inside the hole well while in the conduction band only the first electron state $E1$ is confined inside the well. The $(SQS\text{-}4)_6(InP)_6$ and $(MAs)_6(InP)_6$ superlattices display the same level scheme but only three hole states are confined in the well.

As we will see below, only the first three hole states at the top of the valence band have a high transition probability to the $E1$ state. Of these hole states only the first two, which we name $V1$ and $V2$, contribute to the in-plane PA. This situation is common to all the superlattices considered here. Our attention is devoted to the $V1$ and $V2$ states at the top of the valence band and to the $E1$ electron state at the bottom of the conduction band at the Γ point. We have plotted the squared amplitudes of the planar-averaged wave functions of the $(MAs)_{12}(InP)_{12}$ superlattice (Fig. 3) and of the

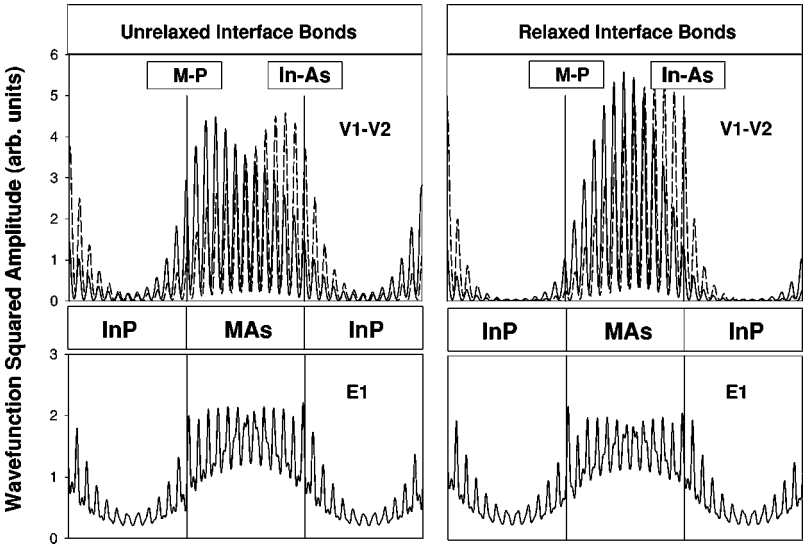

FIG. 3. Wave function squared amplitudes of the hole $V1$ (dashed line) and $V2$ (solid line) states and electron $E1$ state for unrelaxed and relaxed $(MAs)_{12}(InP)_{12}$ superlattice.

$(SQS\text{-}4)_6(InP)_6$ superlattice (Fig. 4) along the superlattice growth direction. The wave functions of the $V1$ and $V2$ hole states are localized inside the MAs well. The localization is higher for the superlattice with period $n=12$ (Fig. 3) than for the superlattice with period $n=6$ (Fig. 4). In both cases the atomic relaxations lead to an increase of the localization of the hole states into the well. In the case of the VCA for the GaInAs alloy (Fig. 3) the relaxation leads to a wave function amplitude of the $V1$ and $V2$ states at the In-As interface larger than at the M-P interface. A similar behavior is not displayed, instead, by the analogous wave functions when the alloy is described by the SQS-4 model (Fig. 4). Looking more carefully at the plots we can see that the sum of the $V1$ and $V2$ amplitudes are always larger at the In-As interface than at the M-P interface. Atomic relaxations increase this trend. The asymmetric behavior of the $V1$ and $V2$ envelopes along z at Γ is a direct consequence of the no-common atom nature of the superlattices. The electron $E1$ state is less localized of the hole states and its localization increases with the superlattice period n.

B. Optical properties: Dielectric tensor and in-plane polarization anisotropy

The anisotropy effects are observed over a 70 meV range,[3] which corresponds to the optical transitions between the upper hole states, localized into the (InGa)As layers, and the first conduction state $E1$, which is also localized into the (InGa)As well. The calculated dielectric tensor elements corresponding to the optical transitions between these states at the Γ point are given in Table II, together with the corresponding transition energies and dipole oscillator strengths. Table II gives the *ab initio* calculated dielectric tensor elements for both the unrelaxed and relaxed $(MAs)_{12}(InP)_{12}$ and $(SQS\text{-}4)_6(InP)_6$ superlattices. Under the entry ''dipole oscillator strength'' we indicate in the table the quantity $|P_{vc}|^2$ which is a measure of the probability of the transition (without considering the direction of the polarization vector). We see that only the transitions from the higher $V1$, $V2$, and $V3$ hole states to the first electron state $E1$, have a substantial probability in the considered energy range. However, only the crystal splitted $V1$ and $V2$ states contribute to the

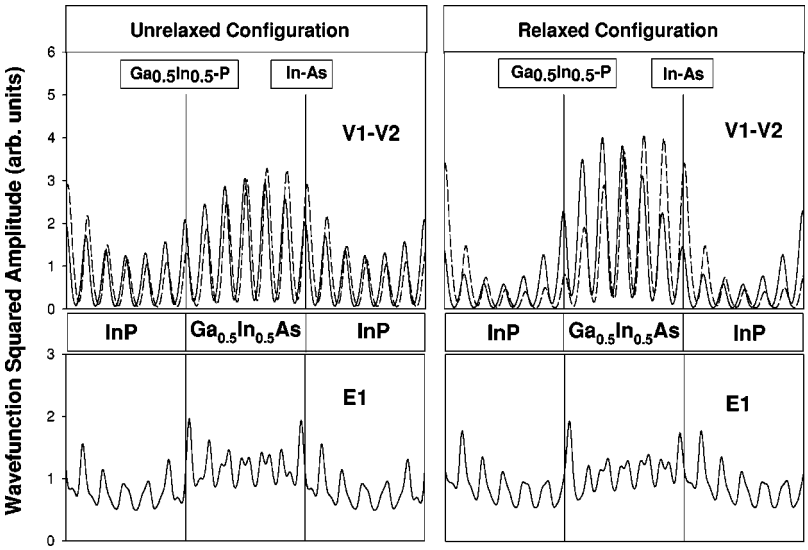

FIG. 4. Wave function squared amplitudes of the hole $V1$ (dashed line) and $V2$ (solid) states and electron $E1$ state for unrelaxed and relaxed $(SQS\text{-}4)_6(InP)_6$ superlattice.

TABLE II. Calculated dielectric tensor elements for the unstrained and strained NCA superlattices.

Transition	Energy (eV)	Dipole oscillator strength	ϵ_{xx}	ϵ_{yy}	ϵ_{zz}	ϵ_{xy}	ϵ_{xz}	ϵ_{yz}
					$(MAs)_{12}(InP)_{12}$ unrelaxed			
$V1$-$E1$	0.6273	0.22047	4.0741	4.0741	0.00	−4.0741	0.00	0.00
$V2$-$E1$	0.6288	0.22217	4.0859	4.0859	0.00	+4.0859	0.00	0.00
$V3$-$E1$	0.6637	0.21537	0.00	0.00	7.1095	0.00	0.00	0.00
$V4$-$E1$	0.6994	0.00741	0.1102	0.1102	0.00	−0.1102	0.00	0.00
$V5$-$E1$	0.7001	0.00674	0.0999	0.0999	0.00	+0.0999	0.00	0.00
					$(MAs)_{12}(InP)_{12}$ relaxed			
$V1$-$E1$	0.5917	0.19746	4.1016	4.1016	0.00	−4.1016	0.00	0.00
$V2$-$E1$	0.6056	0.20724	4.1090	4.1090	0.00	+4.1090	0.00	0.00
$V3$-$E1$	0.6781	0.22033	0.00	0.00	6.9672	0.00	0.00	0.00
$V4$-$E1$	0.6943	0.00832	0.1254	0.1254	0.00	−0.1254	0.00	0.00
$V5$-$E1$	0.7138	0.00085	0.0121	0.0121	0.00	+0.0121	0.00	0.00
					$(SQS\text{-}4)_6(InP)_6$ unrelaxed			
$V1$-$E1$	0.6225	0.22413	4.2057	4.2057	0.00	−4.2057	0.00	0.00
$V2$-$E1$	0.6351	0.23701	4.2684	4.2684	0.0072	+4.2684	0.1749	0.1749
$V3$-$E1$	0.6543	0.23531	0.0039	0.0039	7.9842	0.0039	−0.1763	−0.1763
$V4$-$E1$	0.9043	0.00206	0.0183	0.0183	0.00	−0.0183	0.00	0.00
$V5$-$E1$	0.9137	0.00067	0.0058	0.0058	0.00	+0.0058	0.00	0.00
					$(SQS\text{-}4)_6(InP)_6$ relaxed			
$V1$-$E1$	0.5739	0.19395	4.2813	4.2813	0.00	−4.2813	0.00	0.00
$V2$-$E1$	0.6249	0.21296	3.9571	3.9571	0.0154	+3.9571	0.2464	0.2464
$V3$-$E1$	0.7037	0.23469	0.0065	0.0065	6.8791	0.0065	−0.2113	−0.2113
$V4$-$E1$	0.8492	0.00059	0.0059	0.0059	0.00	−0.0059	0.00	0.00
$V5$-$E1$	0.9273	0.00516	0.0435	0.0435	0.0001	+0.0435	0.0025	0.0025

in-plane absorption since the $V3$-$E1$ transition has oscillator strength components only along the z axis. This behavior of the interband transitions is shared by all the structures considered here.

From the calculated dielectric tensor components we see the following. (1) The in-plane elements are fully decoupled from the elements along the z growth direction. (2) The xy elements of the dielectric tensor relative to the in-plane transitions are different from zero in the case of the NCA superlattices as predicted by theory group symmetry considerations. (3) Very importantly, the elements of the dielectric tensor relative to the two crystal field splitted states $V1$ and $V2$ have almost the same magnitude. (4) The xy elements have the same magnitude of the xx and yy elements. (5) The xy elements of the dielectric tensor relative to the transitions from $V1$ and $V2$ to $E1$ have opposite sign.

These results allow us to study the origin of the dependence of the optical absorption on the polarization vector direction. By considering only the two splitted states at the top of the valence band at the Γ point and indicating with ω_1 and ω_2 the transition energies to the $E1$ state, we have for the absorption anisotropy at these energies [Eq. (8)]

$$\Delta\epsilon_2(\omega_1) = 2\epsilon_{xy}(\omega_1) \tag{9}$$

and an analogous expression for $\Delta\epsilon_2$ at ω_2. Since $\epsilon_{xy}(\omega_1) \sim -\epsilon_{xy}(\omega_2)$ and $|\epsilon_{xy}|$ equals the diagonal elements of the dielectric tensor, we see from Eq. (5) that

$$\epsilon_2\left(\omega_1, \frac{\pi}{4}\right) = 2\epsilon_{xx}(\omega_1) \quad \text{while} \qquad \epsilon_2\left(\omega_2, -\frac{\pi}{4}\right) = 0 \tag{10}$$

or vice versa. An opposite behavior is found for the transition at energy ω_2. Thus, the polarization direction enhances or quenches selectively the optical transitions associated to the C_{2v} crystal field splitted states. In the case of the unrelaxed superlattice with the alloy treated with the VCA, the crystal field splitting ΔE between the transitions $V1$-$E1$ and $V2$-$E1$ differ less than 2 meV. Since the PA is practically *only* due to the small splitting (1.5 meV) $\omega_1 - \omega_2$ between the two CF splitted states, the two transitions fall very close in energy and the anisotropy effects tend to cancel in the absorption spectrum.

The splitting between $V1$ and $V2$ is related to the part of the crystal potential V_a which has a C_{2v} symmetry. Using perturbation theory at the zeroth order approximation

$$|\Delta E| = |\omega_1 - \omega_2| = [(V_{a,xx} - V_{a,yy})^2 - 4(V_{a,xy})^2]^{1/2}. \tag{11}$$

In the case of the (001) grown superlattices $V_{a,xx} = V_{a,yy}$, thus $|\Delta E| = 2|V_{a,xy}|$. The splitting ΔE is a measure of the intensity of the C_2v coupling between the degenerate (in the D_{2d} symmetry) X and Y states at the top of the valence band. At zeroth order $|V1\rangle = |X+Y\rangle$ and $|V2\rangle = |X-Y\rangle$. The symmetry of the valence $V1$ and $V2$ states allows us to interpret the results obtained in Table II easily for the dielectric tensor elements.[17]

The dielectric tensor elements for the relaxed $(MAs)_{12}(InP)_{12}$ superlattice are given in the second part of the Table II. Strain has reduced the fundamental optical gap and opened further the energy gap between the first two in-plane hole states. The splitting is now 13.9 meV. The dielectric tensor elements are almost unchanged because the diminished transition energies are compensated by reduced dipole oscillator strengths. Thus, the *only* difference between the dielectric tensor of the unrelaxed and the relaxed superlattice is the increased energy splitting between the first two interband transitions at ω_1 and at ω_2.

The dielectric tensor elements of the $(SQS\text{-}4)_6(InP)_6$ superlattice are given in the last section of Table II. There are a few important differences with the VCA case. (1) The second and third transitions are not exclusively polarized in-plane or along z, even if the second transition is again *mainly* polarized in the plane and the third transition is *mainly* polarized along the z direction. (2) The splitting between the first two transitions polarized in the xy plane is larger than for the VCA case: 12.6 meV instead of 1.5 meV for the unrelaxed superlattices and 51.0 meV instead of 13.9 meV for the relaxed superlattices. (3) The relaxation pushes the first transition to a lower energy. (4) The difference between the intensity of the two transitions increases with respect to the VCA case. These results show that the C_{2v} part of the superlattice potential is larger when the $Ga_{0.5}In_{0.5}As$ alloy is described using the SQS approach.

Then, we have calculated the absorption coefficient α [Eq. (2)] for the $(MAs)_{12}(InP)_{12}$ superlattice. We have used for the calculation thirteen k points in the IBZ. The calculated $\alpha(\omega)$ has been dressed by a Gaussian broadening of 30 meV. The spectrum for the unrelaxed $(MAs)_{12}(InP)_{12}$ superlattice in the energy range of the two transitions is given in Fig. 5(a), where we see the substantial superposition of the two curves (corresponding to the two polarization directions along $[-110]$ and $[110]$, respectively). The corresponding polarization rate $P(\omega)$, Eq. (1), is small, about 2%. The behavior of $P(\omega)$ in the energy range between the first and second transitions agrees with the experimental result but its value is significantly underestimated. In Fig. 5(b) we show the absorption coefficient relative to the relaxed system. The absorption peaks corresponding to the two transitions are now fully resolved. Again, absorption corresponding to a polarization vector along the 110 direction selects one transition, while absorption corresponding to a polarization vector along -110 ''sees'' only the other transition. The corresponding polarization rate is now larger, about 15%. It is increased by an order of magnitude. Thus, in our model which still neglects spin-orbit interaction, the mechanism of the anisotropy is due entirely to the further crystal field splitting of the $V1$ and $V2$ hole states. We compare the spectrum of Fig. 5(b) with the experimental absorption spectrum given in Fig. 5(c). The experimental result has been rigidly shifted by 325 meV towards lower energies to account for the theoretical LDA underestimation of the fundamental gap. There is an interesting similarity between the two spectra, both in shape and intensity for polarizations along [110] and $[-110]$. The shift between the two absorption features displayed by our calculated spectra are still underestimated (13.9 meV against the experimental value 40 meV). It is interesting to note that the polarization rate is here directly linked to the energy gap between the $V1$ and $V2$ states: a gap of 1.5 meV gives a $p(\omega)$ maximum of $\approx 2\%$, whereas a gap of 13.9 meV increases this value to 15%.

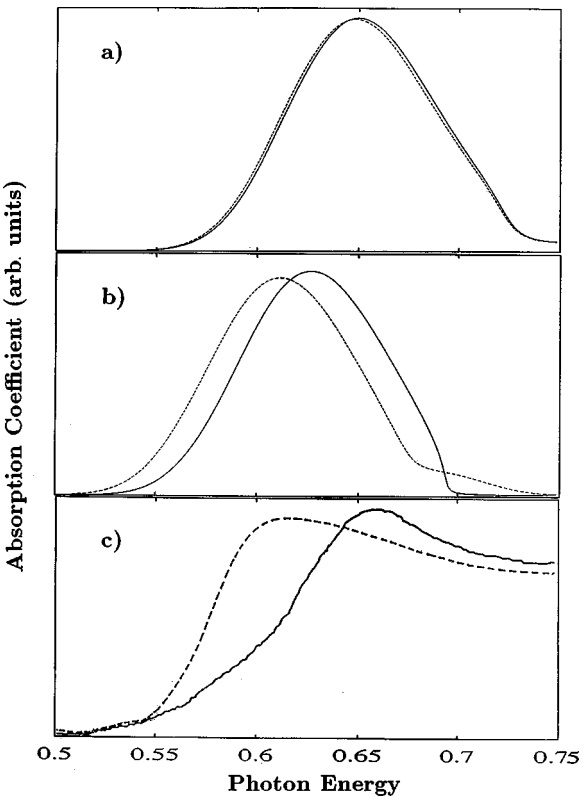

FIG. 5. Calculated absorption spectra for a photon polarization along $[-110]$ (dashed curve) and along [110] (continous curve) for unstrained interfaces (a) and strained (b) interfaces, compared to the experimental results taken from Ref. 3(c).

Finally in Fig. 6 we plot $\epsilon_2(\omega)$ calculated at the Γ point for all the structures. Again a Gaussian broadening 0.3 eV has been used to dress the transitions. We can see the following trends. (i) Shorter the period n of the superlattice higher are the energies of the transitions and larger the splitting between the first and the second transition. (ii) The splitting between $V1$ and $V2$ becomes larger when the system

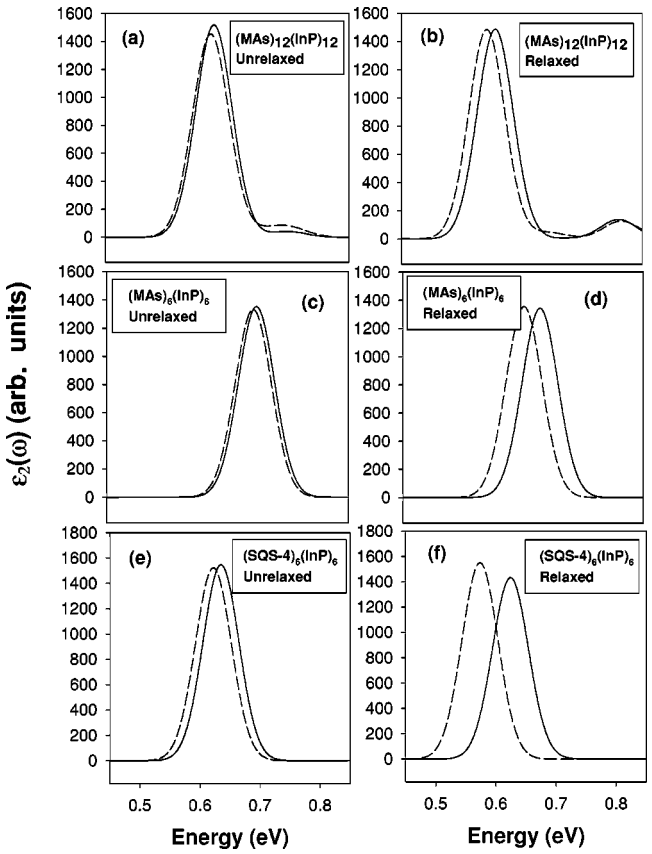

FIG. 6. Imaginary part of the dielectric function $\epsilon_2(\omega)$ for the two polarization directions [110] (solid curve) and [−110] (dashed curve) in the energy range from 0.45 to 0.85 meV. Only the interband transitions at the Γ point have been considered.

relax. (iii) When the true Ga and In cations are taken into account instead of a common M cation [Figs. 6(c) and 6(e)] we obtain an increase of the splitting. Notice that in this case the systems are both unrelaxed, that is the atoms are on the same sites. Thus also the chemical difference between the Ga and In potentials increases the C_{2v} component of the superlattice potential. (iv) The relaxation of the $(SQS\text{-}4)_6(InP)_6$ system leads to an huge splitting of the two transitions, to an enhanced difference in their intensity and to a big shift to lower energies of the transitions [see Fig. 6(f)]. These effects should be contrasted with the results of Fig. 6(d) for the relaxed $(MAs)_6(InP)_6$ where these effects are much smaller. These results show that the ternary nature of the $Ga_{0.}5In_{0.5}As$ constituent has important effects on the absorption spectrum of nanostructures and efforts should be made to fully include it in the theoretical description.

Obviously we have still neglected other important effects in our calculations such as the spin-orbit coupling, and, possibly, a quasiparticle correction to the LDA hole eigenenergies. On the experimental side it is well known that the $H1$-$L1$ splitting is also strongly affected by biaxal tensile strains which we did not include in our calculation.

VI. CONCLUSIONS

In conclusion we have shown how symmetry reduction in NCA superlattices from the D_{2d} to the C_{2v} point group leads to a polarization dependent anisotropy of the optical absorption. Through direct first-principles calculations of the dielectric tensor elements we have found that the polarization direction selects (that is, enhances or quenches) the optical transitions from the crystal field valence states $V1$ and $V2$ to the first $E1$ electron state. This mechanisms gives rise to the observed anisotropy with photon polarization and is likely to be present also in many other systems with broken degeneracies. We have contrasted two different approximations for the alloy $Ga_{0.5}In_{0.5}As$ compound and shown that both the chemical difference and the bulk atomic relaxations due to the true ternary nature of the alloy lead to important effects in the absorption spectrum and in the in-plane PA. Our results suggest also that through manipulation of the interface structure or chemistry or subjecting the system to biaxial in-plane strains (that is, modifying V_a) it is possible to enhance or reduce the polarization dependence of the optical absorption in noncommon atom superlattices.

ACKNOWLEDGMENTS

This work has been carried out within the MURST Project No. COFIN99, the european Project No. INTAS99 and has benefited from collaborations within the Network ''*Ab-initio* (from electronic structure) calculations of complex processes in materials.''

[1] O. Krebs and P. Voisin, Phys. Rev. Lett. **77**, 1829 (1996).
[2] W. Seidel, P. Voisin, J.P. André, and F. Bogani, Solid-State Electron. **40**, 729 (1996).
[3] O. Krebs, W. Seidel, J.P. André, D. Bertho, C. Jouanin, and P. Voisin, Semicond. Sci. Technol. **12**, 938 (1997).
[4] E. Ivchenko, A. Kaminski, and U. Rossler, Phys. Rev. B **54**, 5852 (1996).
[5] O. Krebs, D. Rondi, J.L. Gentner, L. Goldstein, and P. Voisin, Phys. Rev. Lett. **80**, 5770 (1998).
[6] Y. Foulon and C. Priester, Phys. Rev. B **45**, 6259 (1992).
[7] R. Magri and S. Ossicini, Phys. Rev. B **58**, R1742 (1998).
[8] J.F. Cornwell, *Group Theory and Electronic Energy Bands in Solids* (North-Holland, Amsterdam, 1969).
[9] A. Zunger, S.-H. Wei, L.G. Ferreira, and J.E. Bernard, Phys. Rev. Lett. **65**, 353 (1990).
[10] M. Peressi, S. Baroni, A. Baldereschi, and R. Resta, Phys. Rev. B **41**, 12 106 (1990).
[11] G. Kerker, J. Phys. C **13**, L189 (1980).
[12] S.G. Louie, S. Froyen, and M.L. Cohen, Phys. Rev. B **26**, 1738 (1982).
[13] D.M. Ceperley and B.J. Alder, Phys. Rev. Lett. **45**, 566 (1980).
[14] M.S. Hybertsen, Phys. Rev. Lett. **64**, 555 (1990).
[15] R.G. Dandrea, C.B. Duke, and A. Zunger, J. Vac. Sci. Technol. B **10**, 1744 (1992).

[16] *Physics of Group IV Elements and III-V Compounds*, Landolt-Börnstein, Group III, Vol. 17/a (Springer-Verlag, Berlin, 1982).

[17] The cartesian components of the dipole oscillator matrix elements which enter in the definition of the dielectric tensor, Eq. (4), are in this approximation, $P_x(V1\rightarrow E1)=P_x(X\rightarrow E1)$, $P_y(V1\rightarrow E1)=P_y(Y\rightarrow E1)$, $P_x(V2\rightarrow E1)=P_x(X\rightarrow E1)$, $P_y(V2\rightarrow E1)=-P_y(Y\rightarrow E1)$. Applying the results of Table I we obtain that $\epsilon_{xy}(V2\rightarrow E1)=-\epsilon_{xy}(V1\rightarrow E1)$ and $|\epsilon_{xy}|=|\epsilon_{xx}|$ as found in our calculations (Table II).